

# White Spot Syndrome Virus Proteins and Differentially Expressed Host Proteins Identified in Shrimp Epithelium by Shotgun Proteomics and Cleavable Isotope-Coded Affinity Tag<sup>∇†</sup>

Jinlu Wu,<sup>‡</sup> Qingsong Lin,<sup>‡</sup> Teck Kwang Lim, Tiefei Liu, and Choy-Leong Hew\*

Department of Biological Sciences, National University of Singapore, Singapore 117543, Singapore

Received 9 May 2007/Accepted 13 August 2007

Shrimp subcuticular epithelial cells are the initial and major targets of white spot syndrome virus (WSSV) infection. Proteomic studies of WSSV-infected subcuticular epithelium of *Penaeus monodon* were performed through two approaches, namely, subcellular fractionation coupled with shotgun proteomics to identify viral and host proteins and a quantitative time course proteomic analysis using cleavable isotope-coded affinity tags (cICATs) to identify differentially expressed cellular proteins. Peptides were analyzed by offline coupling of two-dimensional liquid chromatography with matrix-assisted laser desorption ionization–tandem time of flight mass spectrometry. We identified 27, 20, and 4 WSSV proteins from cytosolic, nuclear, and membrane fractions, respectively. Twenty-eight unique WSSV proteins with high confidence (total ion confidence interval percentage [CI%], >95%) were observed, 11 of which are reported here for the first time, and 3 of these novel proteins were shown to be viral nonstructural proteins by Western blotting analysis. A first shrimp protein data set containing 1,999 peptides (ion score,  $\geq 20$ ) and 429 proteins (total ion score CI%, >95%) was constructed via shotgun proteomics. We also identified 10 down-regulated proteins and 2 up-regulated proteins from the shrimp epithelial lysate via cICAT analysis. This is the first comprehensive study of WSSV-infected epithelia by proteomics. The 11 novel viral proteins represent the latest addition to our knowledge of the WSSV proteome. Three proteomic data sets consisting of WSSV proteins, epithelial cellular proteins, and differentially expressed cellular proteins generated in the course of WSSV infection provide a new resource for further study of WSSV-shrimp interactions.

White spot syndrome virus (WSSV) has been a catastrophic pathogen of cultured penaeid shrimps since its first appearance in the early 1990s (32). The initial and major target of this virus is shrimp epithelia, including subcuticular, stomach, and gill epithelia. WSSV-infected epithelial cells show hypertrophied nuclei containing massive amounts of viruses (26). Genomic studies revealed that the virus consists of a double-stranded DNA of about 300 kbp with more than 180 predicted open reading frames (ORFs) (9, 43, 54). So far, the majority of proteins encoded by the predicted ORFs have not been detected, and functions of many of these presumptive proteins remain elusive. Information on virus-host interactions is therefore very limited.

Proteomics has been demonstrated to be an important platform technology and has contributed to our understanding of virus-host interaction (4, 37). Shotgun two-dimensional liquid chromatography–tandem mass spectrometry (2D-LC-MS/MS) is a promising approach for high-throughput identification of proteins (21, 48). Cleavable isotope-coded affinity tags (cICATs) coupled with 2D-LC-MS/MS enable the quantitative pairwise comparison of protein expression levels in uninfected and infected cells (7, 15). Previous proteomic studies on WSSV had identified more than 40 viral structural proteins (19, 25, 41, 56),

of which 33 were designated envelope proteins (25, 53). However, our knowledge of viral nonstructural proteins and the host cellular response during WSSV infection remains poor. To date, only a few nonstructural proteins, encoded by highly conserved gene sequences, such as DNA polymerase (9), ribonucleotide reductase (27), and others (14, 16, 18, 27, 28, 47), have been confirmed by traditional gene cloning and immunoassays. Differential expression of host proteins was mainly investigated at the mRNA level using cDNA microarrays and expressed sequence tags (11, 12, 17, 36, 39, 44). Only one investigation on the protein expression profiles of the stomachs of WSSV-infected *Litopenaeus vannamei* shrimp, using 2D gel electrophoresis and MS, has been reported (45). In the present study, we explored WSSV proteins and differentially expressed cellular proteins from WSSV-infected epithelium by using shotgun and cICAT proteomics. We identified 28 viral proteins, including 11 novel viral proteins, 3 of which were confirmed to be nonstructural proteins. We also identified 10 down-regulated and 2 up-regulated cellular proteins. Their potential roles in virus-host interactions are discussed.

## MATERIALS AND METHODS

**Shrimp, virus, and challenge.** Virus inocula were prepared from stored hemolymph of WSSV-infected shrimp and intramuscularly injected into black tiger shrimp (*Penaeus monodon*; body weight, 10 to 15 g), while phosphate-buffered saline (PBS) vehicle was injected in parallel as a control (52). The challenge dose was optimized to ensure 100% mortality within 5 days of infection. The virus infection was confirmed by PCR using a pair of specific primers for WSSV.

**Abundance of viral proteins in different tissues.** The stomach, gill, and epithelium of the cephalothorax subcuticle were sampled from moribund individuals at 3 days postinfection for the extraction of whole-tissue lysates. Briefly, 0.5 g of each sample was homogenized with 1 ml precooled lysis buffer {7 M urea, 2

\* Corresponding author. Mailing address: Department of Biological Sciences, National University of Singapore, Singapore 117543, Singapore. Phone: 65-6516-2692. Fax: 65-6779-5671. E-mail: dbshead@nus.edu.sg.

† Supplemental material for this article may be found at <http://jvi.asm.org/>.

‡ J.W. and Q.L. contributed equally to this work.

∇ Published ahead of print on 22 August 2007.

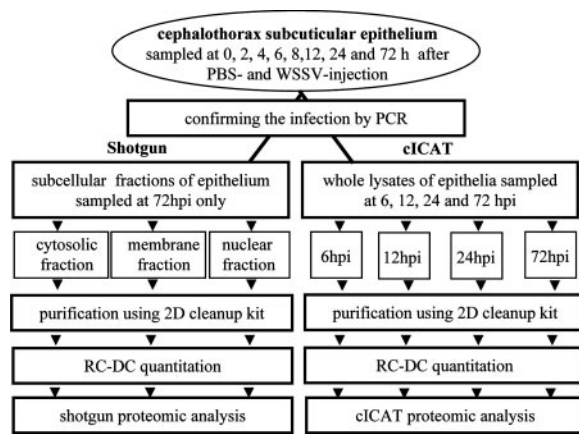


FIG. 1. Workflow for sample collection and sample preparation.

M thiourea, 4% 3-[(3-cholamidopropyl)-dimethylammonio]-1-propanesulfonate (CHAPS), 40 mM Tris base, 2 mM tributylphosphine} and incubated on ice for 10 min. After centrifugation at  $20,000 \times g$  for 20 min at  $4^{\circ}\text{C}$ , the supernatant was treated using a 2-D cleanup kit (GE Healthcare), followed by dissolution in the denaturing buffer (0.1% sodium dodecyl sulfate [SDS], 50 mM Tris, pH 8.5) to keep the proteins under the same conditions as those used for shotgun and cICAT analyses. The protein concentration was determined by RC DC protein assay (Bio-Rad), using bovine  $\gamma$ -globulin as a standard. Equal amounts of proteins (30  $\mu\text{g}$ ) were resolved by SDS-polyacrylamide gel electrophoresis (SDS-PAGE), and the relative abundance of viral proteins was analyzed by Western blotting.

**Sample preparation for shotgun proteomic analysis.** Cephalothorax subcuticular epithelium was sampled at 3 days postinfection. Cytosolic, membrane, and nuclear fractions were sequentially isolated using a Qproteome cell compartment kit (QIAGEN) with the following procedures. Tissue (0.5 g) was washed twice with ice-cold PBS and then homogenized with buffer CE1. After incubation on ice for 10 min, the lysate was centrifuged at  $1,000 \times g$  for 20 min at  $4^{\circ}\text{C}$ . The supernatant (cytosolic fraction) was transferred and stored on ice. The other two fractions were extracted using procedures described in the kit manual. Three fractions were then cleaned and redissolved in the denaturing buffer, followed by the determination of protein concentrations as described previously. Fractionation efficiency was examined by Western blotting before proceeding to trypsin digestion. Four hundred micrograms of proteins from each fraction was reduced with 2 mM triscarboxyethylphosphine and carbamidomethylated using 50 mM iodoacetamide. Porcine trypsin (Applied Biosystems) was added at an estimated enzyme-to-substrate ratio of 1:50 (wt/wt) and incubated overnight at  $37^{\circ}\text{C}$ . A strong-cation-exchange (SCX) column (Applied Biosystems) was used to remove SDS, trypsin, and other reagents from the peptide digestion. Sep-Pak cartridges (Waters) were used for peptide desalting.

**Sample preparation for cICAT analysis.** Cephalothorax subcuticular epithelium were collected at 6, 12, 24, and 72 h postinfection (hpi) from both WSSV- and PBS vehicle-injected individuals for time course cICAT analyses. To minimize deviations arising from individuals, the sample collected at each time point was a pool from five individuals for both the WSSV- and PBS-injected groups. The workflow for sampling and protein preparation is outlined in Fig. 1.

Whole-tissue proteins were extracted and quantitated using the same procedures as those described above for the abundance of viral proteins in different tissues. One hundred micrograms of proteins from the virus- and PBS-injected samples was reduced with 2 mM triscarboxyethylphosphine and labeled with heavy (H) and light (L) cICAT reagents (Applied Biosystems), respectively, for 2 h at  $37^{\circ}\text{C}$  in the dark. Labeled proteins were combined and digested with 25  $\mu\text{g}$  trypsin at  $37^{\circ}\text{C}$  for 16 h, followed by cation-exchange chromatography and avidin affinity purification.

**2D-LC separation of peptide mixtures.** Peptide mixtures for both shotgun and cICAT proteomics were separated using an Ultimate dual-gradient LC system (Dionex-LC Packings) equipped with a Probot matrix-assisted laser desorption ionization (MALDI) spotting device, as follows. The peptide mixture was dissolved in 98%  $\text{H}_2\text{O}$ -2% acetonitrile (ACN) with 0.05% trifluoroacetic acid (TFA) and injected into a 0.3- by 150-mm strong-cation-exchange (SCX) chromatography column (FUS-15-CP; Poros 10S [Dionex-LC Packings]) for first-dimension separation. Mobile phases A and B were 5 mM  $\text{KH}_2\text{PO}_4$  buffer, pH

3, plus 5% ACN and 5 mM  $\text{KH}_2\text{PO}_4$  buffer, pH 3, plus 5% ACN plus 500 mM KCl, respectively. The flow rate for the SCX column was 6  $\mu\text{l}/\text{min}$ . Nine fractions were separated by step gradients of mobile phase B (unbound, 0 to 5%, 5 to 10%, 10 to 15%, 15 to 20%, 20 to 30%, 30 to 40%, 40 to 50%, and 50 to 100%). The eluted fractions were captured alternately on two 0.3- by 1-mm trap columns (3- $\mu\text{m}$   $\text{C}_{18}$  PepMapTM; 100  $\text{\AA}$  [Dionex-LC Packings]) and washed with 0.05% TFA, followed by gradient elution to a 0.2- by 50-mm reverse-phase column (Monolithic PS-DVB; Dionex-LC Packings). Mobile phases A and B used for the second-dimension separation were 98%  $\text{H}_2\text{O}$ -2% ACN with 0.05% TFA and 80%  $\text{H}_2\text{O}$ -20% ACN with 0.04% TFA, respectively. The gradient elution step was 0 to 60% mobile phase B over 15 min at a flow rate of 2.7  $\mu\text{l}/\text{min}$ . The LC fractions were mixed with MALDI matrix solution (7 mg/ml  $\alpha$ -cyano-4-hydroxycinnamic acid and 130  $\mu\text{g}/\text{ml}$  ammonium citrate in 75% ACN) at a flow rate of 5.4  $\mu\text{l}/\text{min}$  through a 25-nl mixing tee (Upchurch Scientific) before being placed as spots onto 192-well stainless steel MALDI target plates (Applied Biosystems, Foster City, CA), using a Probot Micro fraction collector (Dionex-LC Packings) with a speed of 5 s per well.

**MS.** The samples were analyzed by MALDI-tandem time of flight-MS/MS (MALDI-TOF/TOF-MS/MS) (ABI 4700 proteomic analyzer; Applied Biosystems) as previously reported (5). For cICAT samples, ICAT pairs with normalized ratio changes (normalized against the median ratio of all ICAT pairs detected) of  $\geq 40\%$  and the more intense peaks with signal-to-noise ratios of  $\geq 30$  were selected as precursor ions. Singletons with signal-to-noise ratios of  $\geq 50$  were also selected for MS/MS analysis. Raw MS data are accessible via hyperlink at <ftp://dbswjl:dbswjl@137.132.35.227/>.

**Proteomic data analysis.** The MS together with MS/MS spectra were searched using GPS Explorer software, version 3.0, and the MASCOT 2.0 search engine (Matrix Science), allowing one missed cleavage (trypsin). Precursor error tolerance and MS/MS fragment error tolerance were set to 150 ppm and 0.4 Da, respectively. Only fully tryptic peptides with seven amino acids or more and a MS/MS score above 20 were accepted for positive peptide identification.

For protein identification by shotgun proteomics, carbamidomethyl cysteine N-terminal acetylation, pyroglutamation (E or Q), and methionine oxidation were selected as variable modifications. A local database containing all predicted WSSV ORFs (2,013 entries from three complete WSSV genomes [GenBank accession no. AF440570, AF332093, and AF369029]) and the IPI Human Database v. 3.07 (62,322 entries) (<http://www.ebi.ac.uk/IPI/IPIhelp.html>) were used for identification of WSSV proteins. Proteins with a total ion score confidence interval percentage (CI%) above 95% were considered positive identifications. Only a few proteins with total ion score CI% of  $< 95\%$  were checked manually and are presented in Results for reference only. Identified novel viral proteins were further confirmed by Western blotting and/or reverse transcription-PCR (RT-PCR).

An NCBI nr database (4,111,659 entries) was used for host protein identification, but only those peptides with ion scores above 46 (corresponding to total ion score CI% of  $> 50\%$ ) were accepted. All identified cellular proteins were further analyzed using in-house software to group them into either "distinct" proteins [not sharing a peptide(s) with other proteins] or "indistinct" proteins [sharing a peptide(s) with multiple proteins] to clarify possible ambiguous identifications. Unique and shared peptides were numbered and tabulated. If peptides matched multiple members of a protein family, default-setting criteria of MASCOT 2.0 software were used to select the one to be reported. In addition, we randomized the same NCBI nr database by using a perl script downloaded from the Matrix Science website ([http://www.matrixscience.com/help/decoy\\_help.html](http://www.matrixscience.com/help/decoy_help.html)). The same MS and MS/MS data were searched against the randomized database (i.e., decoy database), using the same criteria and software. The numbers of matches, including peptide and protein matches, were counted for the calculation of false-positive rates.

For the analysis of differential expression of cellular proteins by cICAT, an NCBI nr database (4,111,659 entries) was used for the search. H- and L-cICAT-labeled cysteine, N-terminal acetylation, pyroglutamation (E or Q), and methionine oxidation were selected as variable modifications. The maximum peptide rank was set to 1, and the minimum ion score (peptide) was set to 40. cICAT quantification was performed using GPS Explorer v. 3.0 software, and data were normalized against the median ratio obtained from all the ICAT peptide pairs detected in one sample. Cutoff values for protein up-regulation and down-regulation were set at H/L ratios of  $\geq 1.4$  and  $\leq 0.71$ , respectively.

**Time course analysis of 11 novel WSSV protein genes by RT-PCR.** Epithelium was collected in the same way as that described for the cICAT analysis, but with three additional time points, 2, 4, and 8 hpi. Total RNAs were isolated from specimens by using an RNeasy mini kit (QIAGEN). Isolated RNAs (5  $\mu\text{g}$ ) were reverse transcribed with SuperScript III reverse transcriptase and random hexamers (Invitrogen). The first-strand cDNA products were subjected to PCRs

with the primer sets shown in Table SI in the supplemental material. The  $\beta$ -actin transcript was amplified and used as an internal control for RNA quality, efficiency of first-strand cDNA synthesis, and loading amounts for PCRs. One known early gene (*wsv477*) (14) and two structural protein genes (*wsv209* [encoding VP187] and *wsv465* [encoding VP124]) were included for comparison.

**Antibody preparation and Western blotting.** Full-length *wsv051*, *-076*, *-294*, and *-477* genes were cloned into pET-32a (+) vector (Novagen Inc.) and expressed in *Escherichia coli* BL21, and protein expression was confirmed by both DNA sequencing and MALDI-TOF-MS. Purified fusion proteins were subjected to SDS-PAGE analysis prior to immunizing rabbits to generate polyclonal antibodies. Polyclonal antibodies against WSSV VP9, VP26, and VP28 were generated previously (28, 40). Anti-VP664 was kindly provided by C.-F. Lo, National Taiwan University. The following antibodies were purchased: anti-actin (A2066; Sigma), anti-glyceraldehyde-3-phosphate dehydrogenase (anti-GAPDH) (FL-335; Santa Cruz Biotechnology), and anti-histone 2A (H-124; Santa Cruz Biotechnology). Western blotting was carried out as described elsewhere (28).

**Computational annotation.** Topology predictions were performed using the TMHMM predictor ([www.cbs.dtu.dk/services/TMHMM/](http://www.cbs.dtu.dk/services/TMHMM/)), and signal peptide predictions were performed using SignalP3.0 ([www.cbs.dtu.dk/services/SignalP/](http://www.cbs.dtu.dk/services/SignalP/)). Protein families, domains, and functional sites were annotated by searching the InterPro database (<http://www.ebi.ac.uk/InterProScan/>).

## RESULTS

**Identification of WSSV proteins by shotgun proteomics.** Initial experiments were carried out to determine which of the three tissues contained higher concentrations of viral proteins. Western blotting analysis showed that both the structural protein (VP28) and the nonstructural protein (VP9) were more abundant in the subcuticular epithelium and the gill than in the stomach of WSSV-infected shrimp (Fig. 2, left panel). The epithelium was hence chosen for subsequent proteomic analysis.

To improve the identification of viral proteins, cytosolic, nuclear, and membrane fractions were isolated from the epithelium. The efficiency of isolation was examined by Western blotting analysis. The results showed that VP28 and VP9 had the highest concentrations in the cytosolic fraction and the lowest concentrations in the membrane fraction (Fig. 2, right panel). The cellular protein GAPDH, specific to the cytosolic fraction, was the most abundant in the cytosol but could also be detected in the other two fractions. On the other hand, histone 2A, specific to the nuclear fraction, was the most abundant in the nuclear fraction. These results showed that subcellular fractionation could enrich cytosolic and nuclear proteins into their respective fractions.

Twenty-seven, 20, and 4 viral proteins were identified from the cytosolic, nuclear, and membrane fractions, respectively. In total, 33 unique proteins were identified from the three fractions. Twenty-eight of these proteins showed high scores (total ion score CI%, >95%), while the remaining five proteins with low scores (total ion score CI%,  $\leq$ 95%) are also listed (Table 1; see Table SII in the supplemental material). Among the 28 unique proteins, 11 proteins were identified for the first time in this study (shown in bold in Table 1). Of the remaining proteins, there were 13 structural and 4 nonstructural proteins reported previously. Of five proteins with low scores, *wsv226* is reported here for the first time, while the remaining four are previously reported structural proteins. All identified proteins, with either high or low ion scores, have distinct peaks of fragment ions in MS/MS spectra, as found by manual examination. A total of eight proteins were predicted to have transmembrane helices. Four proteins have signal peptides.

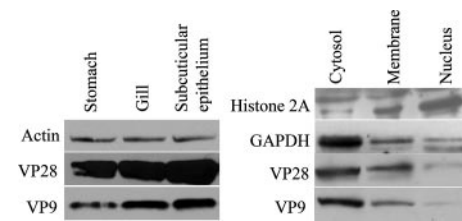


FIG. 2. Relative abundance of viral proteins in different tissues of infected shrimp. (Left) Equal amounts (30  $\mu$ g) of whole lysate proteins extracted from stomachs, gills, and subcuticular epithelia of WSSV-infected shrimp were resolved by SDS-PAGE and then probed with antibodies against  $\beta$ -actin, VP28 (WSSV structural protein), and VP9 (WSSV nonstructural protein), showing that the concentrations of both the structural and nonstructural proteins were relatively higher in the epithelial lysate. (Right) Equal amounts (10  $\mu$ g) of cytosolic, membrane, and nuclear proteins from the epithelium were resolved by SDS-PAGE and probed with antibodies against histone 2A, GAPDH, VP28, and VP9, showing that subcellular fractionation can enrich viral proteins while reducing the nucleus-specific protein histone 2A in the cytosolic fraction.

### Data set of host proteins identified by shotgun proteomics.

To investigate the protein composition of shrimp epithelium, MS and MS/MS spectra from shotgun proteomics of epithelial cytosolic, nuclear, and membrane fractions were combined and searched against an NCBI nr database. A total of 1,999 peptides with ion scores of  $\geq$ 20 were identified, of which 1,669 peptides were identified as having ion scores of  $\geq$ 46 (see Table SIII in the supplemental material). We identified 429 proteins with total ion score CI% of >95%, of which 144 were grouped into "distinct" proteins (see Table SIVa in the supplemental material), while the remaining 285 proteins were grouped into "indistinct" proteins (see Table SIVb in the supplemental material). Using the randomized database, we identified 95 false-positive matches at the peptide level (ion score,  $\geq$ 46) and 9 false-positive matches at the protein level, with total ion score CI% of >95%, which correspond to false-positive rates of 5.7% (i.e., 95 of 1,669 peptides) and 2.1% (i.e., 9 of 429 proteins) for peptide and protein identifications, respectively.

**Data set of differentially expressed host proteins identified by cICAT.** To understand the shrimp response to WSSV infection, subcuticular epithelia of WSSV- and PBS (uninfected control)-injected shrimps were sampled in parallel at 6, 12, 24, and 72 hpi, and whole-tissue lysates were then extracted and prepared for cICAT analysis. A total of 12 proteins showing differential expression were identified at the 95% confidence level (Table 2; see Tables SV and SVII in the supplemental material). As previously noted, peptides from the virus-infected group had an H tag, and peptides from the uninfected group had an L tag. Of the 12 proteins, 10 proteins (83.3% of differentially expressed proteins) were down-regulated (H/L ratio,  $\leq$ 0.71) and 2 proteins were up-regulated (H/L ratio,  $\geq$ 1.4). The means and standard deviations of H/L ratios are shown in Table SVII in the supplemental material. The expression of the clottable protein was identified to be unchanged at 6 and 12 hpi, up-regulated at 24 hpi, and down-regulated at 72 hpi. Of the 10 down-regulated proteins, 1, 2, and 7 of them were identified at 12, 24, and 72 hpi, respectively, showing an increasing number of down-regulated proteins with increasing times of infection. For the two up-regulated proteins, up-reg-

TABLE 1. WSSV proteins identified by shotgun proteomics<sup>a</sup>

Predicted ORF	GI accession no.	Fraction(s) <sup>b</sup>	No. of peptides matched	Best ion score <sup>c</sup>	Total ion score	Total ion CI% <sup>d</sup>	Predicted structure and function <sup>e</sup>	Protein name and reference
<b>wsv277</b>	<b>17158380</b>	<b>C, N</b>	<b>14</b>	<b>C 150</b>	<b>1,131</b>	<b>100</b>	<b>No hits</b>	<b>This study</b>
wsv360	17158462	C, M, N	11	N 105	582	100	No hits	VP664 (14)
wsv421	17158523	C, M, N	4	C 112	301	100	SP	VP28 (14)
wsv230	17158334	C	3	C 151	287	100	No hits	VP9 (33)
<b>wsv051</b>	<b>17158155</b>	<b>C</b>	<b>2</b>	<b>C 94</b>	<b>152</b>	<b>100</b>	<b>No hits</b>	<b>This study</b>
wsv209	17158313	C	3	C 87	174	100	No hits	VP187 (32)
<b>wsv294</b>	<b>17158396</b>	<b>C, N</b>	<b>2</b>	<b>C 90</b>	<b>144</b>	<b>100</b>	<b>No hits</b>	<b>This study</b>
<b>wsv327</b>	<b>17158429</b>	<b>C</b>	<b>1</b>	<b>C 103</b>	<b>103</b>	<b>100</b>	<b>No hits</b>	<b>This study</b>
wsv332	17158434	N	2	N 57	111	100	No hits	VP75 (14)
<b>wsv252</b>	<b>17158355</b>	<b>C, N</b>	<b>1</b>	<b>N 99</b>	<b>99</b>	<b>100</b>	<b>TMH</b>	<b>This study</b>
wsv188	17158292	C	1	C 85	85	100	One TMH	RR2 (17)
wsv465	17158566	C, M, N	2	C 48	85	100	No hits	VP136B (14)
<b>wsv343</b>	<b>17158445</b>	<b>C, N</b>	<b>2</b>	<b>N 50</b>	<b>83</b>	<b>100</b>	<b>NTPase</b>	<b>This study</b>
<b>wsv076</b>	<b>17158180</b>	<b>C</b>	<b>2</b>	<b>C 52</b>	<b>81</b>	<b>100</b>	<b>No hits</b>	<b>This study</b>
wsv289	17158391	C	1	C 44	44	100	No hits	VP190 (16)
<b>wsv285</b>	<b>17158388</b>	<b>N</b>	<b>1</b>	<b>N 61</b>	<b>61</b>	<b>100</b>	<b>No hits</b>	<b>This study</b>
wsv477	17158578	C	2	C 38	58	100	No hits	WSV477 (21)
wsv216	17158320	C, M, N	1	N 57	57	100	One TMH, SP	VP124 (35)
wsv002	17158106	N	1	N 53	53	100	SP	VP24 (14)
wsv308	17158410	N	1	N 50	50	100	No hits	VP51C (14, 15)
wsv011	17158115	C, N	2	C 25	45	100	Three TMH, SP	VP53A (14)
<b>wsv143</b>	<b>17158247</b>	<b>C, N</b>	<b>1</b>	<b>C 34</b>	<b>42</b>	<b>99</b>	<b>HMG domain</b>	<b>This study</b>
wsv172	17158276	C, N	2	C 22	43	99	One TMH	RR1 (17)
wsv254	17158357	N	1	N 43	43	98	No hits	VP36b (14, 15)
wsv415	17158517	C, N	1	C 42	42	98	No hits	VP60B (14, 15)
<b>wsv192</b>	<b>17158296</b>	<b>C</b>	<b>1</b>	<b>C 33</b>	<b>41</b>	<b>98</b>	<b>RNPI, one TMH, recognition motif RNP-1</b>	<b>This study</b>
<b>wsv260</b>	<b>17158363</b>	<b>C, N</b>	<b>1</b>	<b>C 33</b>	<b>37</b>	<b>96</b>	<b>D/E/S-rich</b>	<b>This study</b>
wsv390	17158492	C	1	C 36	36	95	No hits	VP38B (14)
<b>wsv226</b>	<b>17158330</b>	<b>C</b>	<b>2</b>	<b>C 31</b>	<b>37</b>	<b>94</b>	<b>No hits</b>	<b>This study</b>
wsv284	17158387	C	1	C 29	29	72	One TMH, SP	VP13 (14)
wsv311	17158413	C	1	C 27	27	59	One TMH, SP	VP26 (14)
wsv001	17158566	C, N	1	C 27	25	36	No hits	VP180 (14, 15)
wsv242	17158346	N	1	N 23	23	0	No hits	VP41B (14, 15)

<sup>a</sup> Cytosolic, nuclear, and membrane fractions were isolated from WSSV-infected subcuticular epithelium for shotgun 2D-LC-MS/MS analysis. The last five proteins in the list (total ion score CI%, <95%) are not considered confident identifications. Proteins shown in bold were identified for the first time. Details of MS data are shown in Table SII in the supplemental material.

<sup>b</sup> C, M, and N, cytosolic, membrane, and nuclear fractions, respectively.

<sup>c</sup> Proteins that were best identified in the cytosol (C), membrane (M), or nucleus (N), with the highest ion score, total ion score, and total ion score CI%.

<sup>d</sup> The closer the CI% is to 100%, the more likely it is that the protein was correctly identified.

<sup>e</sup> SP, signal peptide, predicted using SignalP3.0 software; TMH, transmembrane helix, predicted using TMHMM-2.0 software; D/E/S, single-letter representations of the amino acids Asp/Glu/Ser.

TABLE 2. Summary of differentially expressed cellular proteins identified by time course cICAT analysis<sup>a</sup>

Direction of regulation and protein name	GenBank accession no.	No. of peptides (6/12/24/72 hpi)	Total ion score (6/12/24/72 hpi)	Total ion score CI% (6/12/24/72 hpi)	Avg ICAT ratio (H/L) (6/12/24/72 hpi)
<b>Down-regulated proteins</b>					
Elongation factor 2	37704007	—/—/—/1	—/—/—/54	—/—/—/98.5	—/—/—/0
Aldehyde dehydrogenase	66514094	—/—/—/1	—/—/—/62	—/—/—/99.8	—/—/—/0.3
Serum albumin	62113341	—/—/1/—	—/—/90/—	—/—/100/—	—/—/0.4/—
Heat shock protein 70	123585	—/—/—/1	—/—/—/50	—/—/—/95.3	—/—/—/0.4
FAMeT	85677401	—/1/—/—	—/55/—/—	—/98.5/—/—	—/0.5/—/—
CiTardbp	70571316	—/—/1/1	—/—/48/64	—/—/96.9/99.8	—/—/1.5/0.4
Beta-hemoglobin	29446	—/—/2/—	—/—/105/—	—/—/100/—	—/—/0.5/—
PACAP	18204192	—/—/—/1	—/—/—/49	—/—/—/94.7	—/—/—/0.6
Elongation factor 1	22128323	—/—/—/1	—/—/—/84	—/—/—/100	—/—/—/0.7
Clottable protein	6601498	2/3/1/3	109/254/69/195	100/100/100/100	0.8/1/1.8/0.6
<b>Up-regulated proteins</b>					
Arginine kinase	46401522	—/—/1/1	—/—/75/100	—/—/100/100	—/—/1.4/1.7
Hemocyanin	7414468	—/2/2/2	—/126/146/226	—/100/100/100	—/1.7/1.6/2.1

<sup>a</sup> Pairs of epithelial lysates from uninfected and WSSV-infected *Peneaus monodon* shrimp at 6, 12, 24, and 72 hpi were prepared for cICAT analyses. Proteins with H/L ratios of <0.71 are regarded as down-regulated, while those with H/L ratios of >1.4 are regarded as up-regulated. Details are shown in Tables SV and SVII in the supplemental material. —, no peptide was detected; 0, only the peptide labeled with the light tag was detected.

TABLE 3. Peptides of tubulin and ATPase groups identified by cICAT analysis<sup>a</sup>

Protein group and peptide sequence (section of Table SVI in the supplemental material)	$M_r$ (exptl)	$M_r$ (calculated)	Score	Expect value	H/L ratio
Tubulin group identified at 24 hpi (1)					
SIQFVDWCPTGFK + ICAT_heavy	1,762.88	1,762.88	56	0.0055	0.97
AYHEQLSVAEITNACFEPA <sup>N</sup> QMVK + ICAT_heavy	2,928.43	2,928.42	83	1.3e-005	1.65
Tubulin group identified at 72 hpi (2)					
EIVHLQTGQCGNQIGTK + ICAT_light	2,052.04	2,052.04	132	2.8e-010	0.60
SIQFVDWCPTGFK + ICAT_light	1,753.83	1,753.85	73	0.00022	0.56
RSIQFVDWCPTGFK + ICAT_light	1,909.95	1,909.95	52	0.029	0.30
AVCMLSNTTAAIEAWAR + ICAT_light	2,034.00	2,034.00	66	0.0013	0.50
TIQFVDWCPTGFK + ICAT_light	1,767.86	1,767.87	68	0.00069	0.53
ATPase group identified at 24 hpi (3)					
IPIFSAAGLPHNEIAAQICR + ICAT_heavy	2,356.27	2,356.28	124	9.8e-010	1.41
KDHSDVSNQLYACYAIGK + ICAT_heavy	2,247.11	2,247.10	45	0.072	2.28
ATPase group identified at 72 hpi (4)					
IPIFSAAGLPHNEIAAQICR + ICAT_light	2,347.24	2,347.25	125	1.5e-009	0.64
KDHSDVSNQLYACYAIGK + ICAT_light	2,238.08	2,238.07	70	0.00045	0.38

<sup>a</sup> Details are shown in Table SVI in the supplemental material.

ulation of hemocyanin was first detected at 12 hpi and lasted to 72 hpi, while up-regulation of arginine kinase was detected only at 72 hpi. Neither down-regulated nor up-regulated proteins were detected at 6 hpi.

Two peptides of the tubulin group were detected at 24 hpi (Table 3; see Tables SVI and SVII in the supplemental material); one peptide was up-regulated (H/L ratio = 1.65), and the other did not change significantly (H/L ratio = 0.97). All peptides of the tubulin group identified at 72 hpi showed down-regulation (H/L ratio, <0.7). The same two peptides of the ATPase group were detected at both 24 and 72 hpi (Table 3; see Tables SV and SVII in the supplemental material); one was up-regulated at 24 hpi (H/L ratio = 2.28) and then down-regulated at 72 hpi (H/L ratio = 0.38), and the other did not change significantly at these two time points.

**Time course analysis of 11 novel WSSV protein genes by RT-PCR.** To investigate temporal gene transcription of 11 novel viral proteins and to provide further evidence of their presence at the mRNA level, a time course semiquantitative RT-PCR was performed, with  $\beta$ -actin as an internal control and three other genes (*wsv209*, *-465*, and *-477*) as positive controls. Among 14 genes, 10 showed increasing mRNA levels with the time course of infection (group 1), 1 showed a constant mRNA level at all time points (group 2), and 3 showed decreasing mRNA levels with the time course of infection (group 3) (Fig. 3). On the other hand, six genes (*wsv076*, *-192*, *-143*, *-277*, *-343*, and *-477*) commenced their expression at a very early stage of the infection (2 hpi), while two genes (*wsv285* and *-294*) commenced expression at a later stage of the infection (24 hpi).

**Western blotting.** Western blotting analysis was performed to verify the presence of proteins in the virus-infected tissue and in the purified virus. Four proteins (*wsv051*, *-076*, and *-294* and a known nonstructural viral protein, *wsv477*, as a positive control) were detected in the virus-infected whole-tissue lysate and the cytosolic fraction but were not detected in the purified virus and the uninfected cell lysate (Fig. 4). Positive controls using known viral structural proteins, including

envelope proteins VP28 and VP26 as well as the nucleocapsid protein (VP664), showed that these known structural proteins were present in both tissue lysates and purified virus. The results indicated that the three novel proteins, i.e., *wsv051*, *-076*, and *-294*, might not be viral structural proteins.

## DISCUSSION

The development of proteomic technologies has revolutionized our ability to analyze protein compositions of viruses and

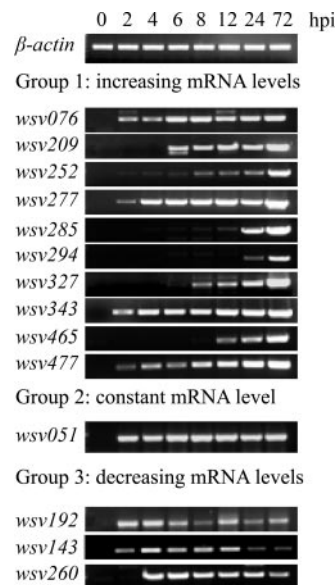


FIG. 3. Temporal transcription of 11 novel viral protein genes. mRNAs were extracted from subcuticular epithelia sampled at 0, 2, 4, 6, 8, 12, 24, and 72 hpi. cDNAs were synthesized using random hexamers and normalized to equal concentrations by  $\beta$ -actin. As the time of infection elapsed, 10 of 14 genes showed increasing mRNA levels (group 1), 1 maintained a constant mRNA level (group 2), and 3 showed decreasing mRNA levels (group 3).

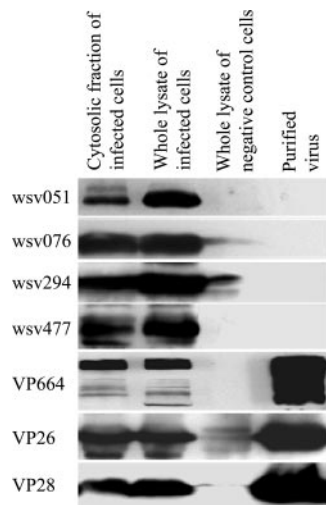


FIG. 4. Western blotting analysis of novel viral proteins. Three novel proteins were present in the total cell lysate and the cytosolic fraction of WSSV-infected epithelia but were not detected in the purified virus and the uninfected cell lysate by Western blotting using antibodies against wsv051, -076, -294, and -477 (a control for viral nonstructural proteins). Viral structural proteins, including the capsid protein VP664 and the envelope proteins (VP28 and VP26), were present in the infected cell lysate and the purified virus.

host protein changes on a global scale, but there are limitations to identifying low-abundance proteins and dynamics of proteins in a single-step procedure or approach (30). We used two complementary proteomic approaches, i.e., shotgun proteomics and iCAT analysis, to analyze virus-infected cells. Coupling effective protein and peptide fractionation technologies with highly sensitive shotgun MS enables the identification of low-abundance proteins, while a time course quantitative analysis using iCAT can reveal the dynamic alternations in cellular protein profiles, deepening our understanding of how the cellular machinery is affected.

Compared with the virion proteome, virus-infected cells have much more complex protein compositions. Two major challenges for the identification of viral proteins from infected cells by shotgun proteomics are how to enrich the viral proteins while reducing the presence of highly abundant cellular proteins (e.g., housekeeping proteins) and how to effectively separate the enormous number of peptides. To enhance the viral protein identification, we undertook the following strategies: (i) finding a tissue type which contained a relatively high level of viral proteins, (ii) reducing the complexity of protein extracts by sequentially isolating three subcellular fractions, and (iii) separating peptides by high-performance 2D-LC (48). Several commercial kits were tested to isolate cytosolic, nuclear, and membrane fractions, none of which could completely eliminate the cross-contamination among the three fractions (data not shown). Nonetheless, the subcellular fractionation did reduce the complexity of host cellular proteins (Fig. 2, right panel). Proteomic analyses of these three fractions identified 28 unique viral proteins, 11 of which were identified for the first time with high confidence. Since these 11 proteins have never been identified previously from 1D and 2D protein gels with purified WSSV, they were tentatively assumed to be candidate nonstructural proteins. Three of these 11 candidates

have been confirmed to be real viral nonstructural proteins by Western blotting analysis. We also tabulated the five proteins with low ion scores (Table 1) for reference only, as they all had distinct MS/MS peptide fragment peaks (see Table SII in the supplemental material). Low ion scores might be related to the low abundance of these viral proteins in the sample and possibly also to other factors. Overall, this study represents an effective strategy for exploring viral proteins from an infected host protein extract, showing its advantage over previous virion proteomics in exploring viral nonstructural proteins.

In addition, we carried out shotgun and iTRAQ proteomic studies of purified WSSV with the aim of assigning the structural proteins into two categories, i.e., envelope and nucleocapsid proteins (25). A novel protein, wsv143, reported in this study was also identified in purified WSSV by shotgun proteomics. Since shotgun proteomics is sensitive in detecting small amounts of proteins and wsv143 was not identified in 1D and 2D gels with purified WSSV proteins, this protein may not be a viral structural protein but may be present in contaminated cell debris which was copurified with WSSV particles.

A time course RT-PCR analysis of the transcription of the 11 novel protein genes showed that they had different transcriptional profiles. Early-transcribed genes might be involved in viral replication and the modification of host cellular metabolism from the very beginning of infection (2 hpi). On the other hand, late-transcribed genes might be involved in virus assembly, maturation, and release. Computational annotation of 11 proteins through an InterPro database search revealed that three of these proteins have homology to known functional domains, which are briefly stated below.

The wsv143 protein has homology to SOX (*Sry box*) proteins (protein family ID, PTHR10270), which contain a high-mobility-group domain allowing them to bind to gene promoters or enhancers and to function as transcription factors (49, 50). The wsv252 protein is the first member of the DUF1335 protein family identified at the protein level (43) and may be involved in DNA replication (23). The wsv343 protein matched a P loop containing nucleoside triphosphate hydrolases (NTPases) (SSF52540). Targeted reduction or point mutants of NTPase inhibit *Toxoplasma gondii* proliferation (31) and viral DNA replication (20). Small molecules designed to inhibit NTPase function may be promising antiviral drugs (3, 8, 34, 38).

Human epithelial proteomics has provided powerful information on the relationships between biological molecules and disease mechanisms (58). Here we have generated a data set of shrimp epithelial proteins through shotgun proteomics. This data set is important not only for studying host-pathogen interactions but also for comparative biology. One problem encountered in generating such a data set is that the same peptide sequence can be present in multiple different proteins or protein isoforms. Shared peptides can therefore lead to ambiguities in determining the identities of proteins (33). To avoid those ambiguities, we developed in-house software by which we classified identified proteins into two groups, i.e., “distinct” proteins, containing peptides which are not shared with others, and “indistinct” proteins, containing peptides that are shared among multiple proteins. For “indistinct” proteins, additional

information, such as molecular weight and gene sequence, is needed for correct identification. This is a shortcoming of shotgun proteomics.

We further carried out a time course cICAT analysis in an attempt to investigate the dynamic changes of host cellular proteins during WSSV infection. The combination of chromatography and cICAT labeling can produce comprehensive information on protein composition and provide accurate quantitation on a subset of proteins (15). The limited number of proteins identified as being expressed differentially in the present study was due mainly to the lack of sequence information for the shrimp genome. Once the genome of shrimp has been sequenced, we will perform the database search again, expecting to identify many more changes in host proteins. The implications of these changes in protein abundance and presumed functional alterations in the context of virus pathogenesis will require further bioinformatic analysis and/or experimental investigations. However, we discuss here a partial selection of host proteins undergoing changes to highlight the importance of further validation and an in-depth study of these proteins.

An increasing number of down-regulated proteins were detected with the elapsing time of infection (zero, one, two, and seven down-regulated proteins at 6, 12, 24, and 72 hpi, respectively). Farnesoic acid *O*-methyltransferase (FAMeT), which may be involved in gametogenesis, oocyte maturation, development, and metamorphosis of shrimp (13, 24), was a down-regulated protein. Down-regulation of FAMeT hints that WSSV infection might regulate, either directly or indirectly, host hormonal systems, growth, and maturation.

Down-regulation of proapoptotic caspase adaptor protein (PACAP) was detected at 72 hpi. PACAP has been demonstrated to exhibit specific binding to caspase-2 and -9, but not to caspase-3, -4, -7, or -8, in 293T cells. Up-regulation of PACAP in human B-cell lines triggered apoptosis (6). WSSV infection could cause a high rate of apoptosis in the shrimp lymphoid organ, but no apoptotic cells were observed in epithelial cells, in which WSSV massively replicated (51). It will be important to determine whether the down-regulation of PACAP in epithelial cells plays a role in suppressing apoptosis and benefiting WSSV replication.

CiTardbp (*Ciona intestinalis* trans-activation-responsive DNA binding protein), which may be involved in mRNA maturation and stabilization, was also down-regulated. Sequence comparison of CiTardbp and the longest isoforms of human, *Drosophila melanogaster*, and *Caenorhabditis elegans* TDP43 (*Tar* DNA binding protein) showed that the highest degree of similarity among the four proteins resides in RNA recognition motif 1 (RRM1) and RRM2 (see Fig. S1 in the supplemental material) (1, 46). TDP43 belongs to the family of heterogeneous nuclear ribonucleoproteins, characterized by binding to RNA and, in some cases, DNA sequences through RRM and participating in a variety of processes, such as RNA transportation, stabilization, and modification, pre-mRNA splicing, and transcriptional regulation (22, 46). It was demonstrated that host cellular TDP43 could interact with the human immunodeficiency virus Tat protein and modulate human immunodeficiency virus type 1 gene expression (35, 50). How the WSSV protein(s) interacts with shrimp cellular TDP43 remains to be determined.

Down-regulation of elongation factor, a heat shock protein (Hsp70), tubulin, and ATPase may represent defects in protein synthesis, folding, and transportation. However, since the peptides identified are common in multiple isoforms of the tubulin family, the cICAT study was unable to tell us which isoforms undergo changes in abundance. Therefore, we determined the H/L ratios of the individual peptides identified as an indication of the overall change in the tubulin family. The change in the ATPase family is shown in the same way.

WSSV infection causing up-regulation of hemocyanin has been investigated previously by transcriptional analysis (11, 12). Our cICAT results show for the first time that the protein level of hemocyanin is up-regulated from 12 hpi. Hemocyanin functions as an immunoglobulin superfamily molecule (57) and is one of the important host factors against pathogenic invasion (2). WSSV infection could induce the aggregation of hemocytes to sites of infection (42). Higher levels of hemocyanin in the epithelium may hint at an antiviral defense mechanism of the shrimp. It is also worth noting that the clottable protein was up-regulated at 24 hpi but dramatically down-regulated at 72 hpi. Since the clottable protein is involved in type C coagulation and biodefense (10, 55), its up-regulation in the early stage of infection may indicate an innate immune response, but its down-regulation in the late stage of infection gives the first experimental data which may explain, at least partially, why hemolymph from shrimp at the late stage of WSSV infection does not coagulate.

In summary, we have developed a general strategy for comprehensive analysis of a large protein complex of virus-infected cells and have shown its successful application to the study of WSSV-infected shrimp epithelia. We identified 11 novel viral proteins, 429 cellular proteins, and 12 differentially expressed cellular proteins. Although the number of cellular proteins identified was limited due to the limitations in shrimp genome data, our research has opened a new venue to further study virus-host interactions and has provided useful data for comparison with different experimental approaches.

#### ACKNOWLEDGMENTS

We thank Shashikant B. Joshi for a critical reading of the manuscript and Zhuang Ying for help with Western blotting analysis.

This work was supported by grants R-154-000-233-112 and R-154-000-255-112 from the Academic Research Council of the National University of Singapore to Choy-Leong Hew.

#### REFERENCES

1. Ayala, Y. M., S. Pantano, A. D'Ambrogio, E. Buratti, A. Brindisi, C. Marchetti, M. Romano, and F. E. Baralle. 2005. Human, *Drosophila*, and *C. elegans* TDP43: nucleic acid binding properties and splicing regulatory function. *J. Mol. Biol.* **348**:575–588.
2. Bachère, E., E. Mialhe, D. Noël, V. Boulo, A. Morvan, and J. Rodriguez. 1995. Knowledge and research prospects in the marine mollusk and crustacean immunology. *Aquaculture* **132**:17–32.
3. Balzarini, J. 2000. Effect of antimetabolite drugs of nucleotide metabolism on the anti-human immunodeficiency virus activity of nucleoside reverse transcriptase inhibitors. *Pharmacol. Ther.* **87**:175–187.
4. Bernhard, O. K., R. J. Diefenbach, and A. L. Cunningham. 2005. New insights into viral structure and virus-cell interactions through proteomics. *Expert Rev. Proteomics* **2**:577–588.
5. Bi, X., Q. Lin, T. W. Foo, S. Joshi, T. You, H. M. Shen, C. N. Ong, P. Y. Cheah, K. W. Eu, and C. L. Hew. 2006. Proteomics analysis of colorectal cancer reveals alterations in metabolic pathways: mechanism of tumorigenesis. *Mol. Cell. Proteomics* **5**:1119–1130.
6. Bonfoco, E., E. Li, F. Kolbinger, and N. R. Cooper. 2001. Characterization of

- a novel proapoptotic caspase-2- and caspase-9-binding protein. *J. Biol. Chem.* **276**:29242–29250.
7. Booy, A. T., J. D. Haddow, L. B. Ohlund, D. B. Hardie, and R. W. Olafson. 2005. Application of isotope coded affinity tag (ICAT) analysis for the identification of differentially expressed proteins following infection of Atlantic salmon (*Salmo salar*) with infectious hematopoietic necrosis virus (IHNV) or *Renibacterium salmoninarum* (BKD). *J. Proteome Res.* **4**:325–334.
  8. Bretner, M., A. Baier, K. Kopanska, A. Najda, A. Schoof, M. Reinholz, A. Lipniacki, A. Piasek, T. Kulikowski, and P. Borowski. 2005. Synthesis and biological activity of 1H-benzotriazole and 1H-benzimidazole analogues—inhibitors of the NTPase/helicase of HCV and of some related Flaviviridae. *Antivir. Chem. Chemother.* **16**:315–326.
  9. Chen, L. L., H. C. Wang, C. J. Huang, S. E. Peng, Y. G. Chen, S. J. Lin, W. Y. Chen, C. F. Dai, H. T. Yu, C. H. Wang, C. F. Lo, and G. H. Kou. 2002. Transcriptional analysis of the DNA polymerase gene of shrimp white spot syndrome virus. *Virology* **301**:136–147.
  10. Chen, M. Y., K. Y. Hu, C. C. Huang, and Y. L. Song. 2005. More than one type of transglutaminase in invertebrates? A second type of transglutaminase is involved in shrimp coagulation. *Dev. Comp. Immunol.* **29**:1003–1016.
  11. Dhar, A. K., A. Dettori, M. M. Roux, K. R. Klimpel, and B. Read. 2003. Identification of differentially expressed genes in shrimp (*Penaeus stylirostris*) infected with white spot syndrome virus by cDNA microarrays. *Arch. Virol.* **148**:2381–2396.
  12. Gross, P. S., T. C. Bartlett, C. L. Browdy, R. W. Chapman, and G. W. Warr. 2001. Immune gene discovery by expressed sequence tag analysis of hemocytes and hepatopancreas in the Pacific white shrimp, *Litopenaeus vannamei*, and the Atlantic white shrimp, *L. setiferus*. *Dev. Comp. Immunol.* **25**:565–577.
  13. Gunawardene, Y. I. N. S., S. S. Tobe, W. G. Bendena, B. K. C. Chow, K. J. Yagi, and S. M. Chan. 2002. Function and cellular localization of farnesoic acid O-methyltransferase (FAMeT) in the shrimp, *Metapenaeus ensis*. *Eur. J. Biochem.* **269**:3587–3595.
  14. Han, F., J. Xu, and X. Zhang. 2007. Characterization of an early gene (wsv477) from shrimp white spot syndrome virus (WSSV). *Virus Genes* **34**:193–198.
  15. Hansen, K. C., S. U. Gerold, R. J. Chalkley, J. Hirsch, M. A. Baldwin, and A. L. Burlingame. 2003. Mass spectrometric analysis of protein mixtures at low levels using cleavable <sup>13</sup>C-isotope-coded affinity tag and multidimensional chromatography. *Mol. Cell. Proteomics* **2**:299–314.
  16. He, F., B. J. Fenner, A. K. Godwin, and J. Kwang. 2006. White spot syndrome virus open reading frame 222 encodes a viral E3 ligase and mediates degradation of a host tumor suppressor via ubiquitination. *J. Virol.* **80**:3884–3892.
  17. He, N., Q. Qin, and X. Xu. 2005. Differential profile of genes expressed in hemocytes of white spot syndrome virus-resistant shrimp (*Penaeus japonicus*) by combining suppression subtractive hybridization and differential hybridization. *Antivir. Res.* **66**:39–45.
  18. Hossain, M. S., S. Khadjjah, and J. Kwang. 2004. Characterization of ORF89—a latency-related gene of white spot syndrome virus. *Virology* **325**:106–115.
  19. Huang, C., X. Zhang, Q. Lin, X. Xu, Z. Hu, and C. L. Hew. 2002. Proteomic analysis of shrimp white spot syndrome viral proteins and characterization of a novel envelope protein VP466. *Mol. Cell. Proteomics* **1**:223–231.
  20. Kahn, J. S., and M. Esteban. 1990. Identification of the point mutations in two vaccinia virus nucleoside triphosphate phosphohydrolase I temperature-sensitive mutants and role of this DNA-dependent ATPase enzyme in virus gene expression. *Virology* **174**:459–471.
  21. Kislinger, T., B. Cox, A. Kannan, C. Chung, P. Hu, A. Ignatchenko, M. S. Scott, A. O. Gramolini, Q. Morris, M. T. Hallett, J. Rossant, T. R. Hughes, B. Frey, and A. Emili. 2006. Global survey of organ and organelle protein expression in mouse: combined proteomic and transcriptomic profiling. *Cell* **125**:173–186.
  22. Krecic, A. M., and M. S. Swanson. 1999. hnRNP complexes: composition, structure, and function. *Curr. Opin. Cell Biol.* **11**:363–371.
  23. Krell, P. J. 1996. Passage effect of virus infection in insect cells. *Cytotechnology* **20**:125–137.
  24. Laufer, H., D. W. Borst, F. C. Baker, M. Carrasco, M. Sinkus, C. C. Reuter, L. W. Tsai, and D. A. Schooley. 1987. Identification of a juvenile hormone-like compound in crustacean. *Science* **235**:202–205.
  25. Li, Z., Q. Lin, J. Chen, J. L. Wu, T. K. Lim, S. S. Loh, X. Tang, and C. L. Hew. 2007. Shotgun identification of structural proteome of shrimp white spot syndrome virus and iTRAQ differentiation of envelope and nucleocapsid subproteomes. *Mol. Cell. Proteomics* **6**:1609–1620.
  26. Lightner, D. V. 1996. A handbook of pathology and diagnostic procedures for diseases of penaeid shrimp. World Aquaculture Society, Baton Rouge, LA.
  27. Lin, S. T., Y. S. Chang, H. C. Wang, H. F. Tzeng, Z. F. Chang, J. Y. Lin, C. H. Wang, C. F. Lo, and G. H. Kou. 2002. Ribonucleotide reductase of shrimp white spot syndrome virus (WSSV): expression and enzymatic activity in a baculovirus/insect cell system and WSSV-infected shrimp. *Virology* **304**:282–290.
  28. Liu, Y., J. Wu, J. Song, J. Sivaraman, and C. L. Hew. 2006. Identification of a novel nonstructural protein, VP9, from white spot syndrome virus: its structure reveals a ferredoxin fold with specific metal binding sites. *J. Virol.* **80**:10419–10427.
  29. Reference deleted.
  30. Maxwell, K. L., and L. Frappier. 2007. Viral proteomics. *Microbiol. Mol. Biol. Rev.* **71**:398–411.
  31. Nakaar, V., B. U. Samuel, E. O. Ngo, and K. A. Joiner. 1999. Targeted reduction of nucleoside triphosphate hydrolase by antisense RNA inhibits *Toxoplasma gondii* proliferation. *J. Biol. Chem.* **274**:5083–5087.
  32. Naylor, R. L., R. J. Goldberg, H. Mooney, M. Beveridge, J. Clay, C. Folke, N. Kautsky, J. Lubchenco, J. Primavera, and M. Williams. 1998. Nature's 10 subsidies to shrimp and salmon farming. *Science* **282**:883–884.
  33. Nesvizhskii, I. A., and R. Aebersold. 2005. Interpretation of shotgun proteomic data—the protein inference problem. *Mol. Cell. Proteomics* **4**:1419–1440.
  34. Neyts, J., A. Meerbach, P. McKenna, and E. De Clercq. 1996. Use of the yellow fever virus vaccine strain 17D for the study of strategies for the treatment of yellow fever virus infections. *Antivir. Res.* **30**:125–132.
  35. Ou, S. H., F. Wu, D. Harrich, L. F. Garcia-Martinez, and R. B. Gaynor. 1995. Cloning and characterization of a novel cellular protein, TDP-43, that binds to human immunodeficiency virus type 1 TAR DNA sequence motifs. *J. Virol.* **69**:3584–3596.
  36. Pan, D., N. He, Z. Yang, H. Liu, and X. Xu. 2005. Differential gene expression profile in hepatopancreas of WSSV-resistant shrimp (*Penaeus japonicus*) by suppression subtractive hybridization. *Dev. Comp. Immunol.* **29**:103–112.
  37. Ravichandran, V., and E. O. Major. 2006. Viral proteomics: a promising approach for understanding JC virus tropism. *Proteomics* **6**:5628–5636.
  38. Ray, A. S. 2005. Intracellular interactions between nucleos(t)ide inhibitors of HIV reverse transcriptase. *AIDS Rev.* **7**:113–125.
  39. Reyes, A., M. Salazar, and C. Granja. 2007. Temperature modifies gene expression in subcuticular epithelial cells of white spot syndrome virus-infected *Litopenaeus vannamei*. *Dev. Comp. Immunol.* **31**:23–29.
  40. Tang, X., J. Wu, J. Sivaraman, and C. L. Hew. 2007. Crystal structure of major envelope proteins VP26 and VP28 from white spot syndrome virus shed light on their evolutionary relationship. *J. Virol.* **81**:6709–6717.
  41. Tsai, J. M., H. C. Wang, J. H. Leu, H. H. Hsiao, A. H. J. Wang, G. H. Kou, and C. F. Lo. 2004. Genomic and proteomic analysis of thirty-nine structural proteins of shrimp white spot syndrome virus. *J. Virol.* **78**:11360–11370.
  42. van de Braak, C. B., M. H. Botterblom, E. A. Huisman, J. H. Rombout, and W. P. van der Knaap. 2002. Preliminary study on haemocyte response to white spot syndrome virus infection in black tiger shrimp *Penaeus monodon*. *Dis. Aquat. Organ.* **51**:149–155.
  43. Van Hulten, M. C. W., J. Witteveldt, S. Peters, N. Kloosterboer, R. Tarchini, M. Fiers, H. Sandbrink, R. K. Lankhorst, and J. M. Vlak. 2001. The white spot syndrome virus DNA genome sequence. *Virology* **286**:7–22.
  44. Wang, B., F. Li, B. Dong, X. Zhang, C. Zhang, and J. Xiang. 2006. Discovery of the genes in response to white spot syndrome virus (WSSV) infection in *Fenneropenaeus chinensis* through cDNA microarray. *Mar. Biotechnol.* **8**:491–500.
  45. Wang, H.-C., H.-C. Wang, J. H. Leu, G. H. Kou, A. H. Wang, and C. F. Lo. 2007. Protein expression profiling of the shrimp cellular response to white spot syndrome virus infection. *Dev. Comp. Immunol.* **31**:672–686.
  46. Wang, H.-Y., I.-F. Wang, J. Bose, and C.-K. J. Shena. 2004. Structural diversity and functional implications of the eukaryotic TDP gene family. *Genomics* **83**:130–139.
  47. Wang, Z., H. K. Chua, A. A. Gusti, F. He, B. Fenner, I. Manopo, H. Wang, and J. Kwang. 2005. RING-H2 protein WSSV249 from white spot syndrome virus sequesters a shrimp ubiquitin-conjugating enzyme, PvUbc, for viral pathogenesis. *J. Virol.* **79**:8764–8772.
  48. Wienkoop, S., M. Glinski, N. Tanaka, V. Tolstikov, O. Fiehn, and W. Weckwerth. 2004. Linking protein fractionation with multidimensional monolithic reversed-phase peptide chromatography/mass spectrometry enhances protein identification from complex mixtures even in the presence of abundant proteins. *Rapid Commun. Mass Spectrom.* **18**:643–650.
  49. Wilson, M., and P. Koopman. 2002. Matching SOX: partner proteins and co-factors of the SOX family of transcriptional regulators. *Curr. Opin. Genet. Dev.* **12**:441–446.
  50. Wissmuller, S., T. Kosian, M. Wolf, M. Finzsch, and M. Wegner. 2006. The high-mobility-group domain of Sox proteins interacts with DNA-binding domains of many transcription factors. *Nucleic Acids Res.* **34**:1735–1744.
  51. Wu, J. L., and K. Muroga. 2004. Apoptosis does not play an important role in the resistance of 'immune' *Penaeus japonicus* against white spot syndrome virus. *J. Fish Dis.* **27**:15–21.
  52. Wu, J. L., K. Suzuki, M. Arimoto, T. Nishizawa, and K. Muroga. 2002. Preparation of an inoculum of white spot syndrome virus for challenge tests in *Penaeus japonicus*. *Fish Pathol.* **37**:65–69.
  53. Xie, X., L. Xu, and F. Yang. 2006. Proteomic analysis of the major envelope and nucleocapsid proteins of white spot syndrome virus. *J. Virol.* **80**:10615–10623.
  54. Yang, F., J. He, X. Lin, Q. Li, D. Pan, X. Zhang, and X. Xu. 2001. Complete genome sequence of the shrimp white spot bacilliform virus. *J. Virol.* **75**:11811–11820.
  55. Yeh, M. S., C. J. Huang, J. H. Leu, Y. C. Lee, and I. H. Tsai. 1999. Molecular

- cloning and characterization of a hemolymph clottable protein from tiger shrimp (*Penaeus monodon*). *Eur. J. Biochem.* **266**:624–633.
56. **Zhang, X., C. Huang, X. Tang, Y. Zhuang, and C. L. Hew.** 2004. Identification of structural proteins from shrimp white spot syndrome (WSSV) by 2 DE-MS. *Proteins* **55**:229–235.
57. **Zhang, Y., S. Wang, A. Xu, J. Chen, B. Lin, and X. Peng.** 2006. Affinity proteomic approach for identification of an IgA-like protein in *Litopenaeus vannamei* and study on its agglutination characterization. *J. Proteome Res.* **5**:815–821.
58. **Zhao, H., B. K. Adler, C. Bai, F. Tang, and X. Wang.** 2006. Epithelial proteomics in multiple organs and tissues: similarities and variations between cells, organs, and diseases. *J. Proteome Res.* **5**:743–755.